Available online at www.sciencedirect.com
SCIENCE DIRECT®
Journal of Organometallic Chemistry 690 (2005) 6054–6067
Journal of Organometallic Chemistry
www.elsevier.com/locate/jorganchem

Oxidative addition of aryl chlorides to palladium N-heterocyclic carbene complexes and their role in catalytic arylamination

Jennifer C. Green *, Benjamin J. Herbert, Richard Lonsdale

Chemistry Department, University of Oxford, Inorganic Chemistry Laboratory, South Parks Road, Oxford OX1 3QR, UK

Received 30 June 2005; received in revised form 30 July 2005; accepted 30 July 2005
Available online 27 September 2005

Abstract

Density functional theory has been used to investigate various solvated species that may be formed from palladium bis N-heterocyclic carbene complexes, [Pd(*cyclo*-C{NRCH}$_2$)$_2$], (PdL$_2$) in benzene solution. Formation of an η^2-arene complex is shown to stabilise a monocarbene species, PdL(η^2-C$_6$H$_5$X), where the arene is either the solvent or a reacting aryl halide. Oxidative addition of an aryl chloride has been modelled, and the most likely transition state has been established as a PdL(arylchloride) species, with just one carbene ligand coordinated to the palladium. The catalytic cycle for aryl amination has been investigated and the oxidative addition of the aryl halide shown to be the rate determining step. Reductive elimination of the aryl amine has a lower activation energy. Oxidative addition of alkyl halides has been shown to be less favourable because of the absence of an unsaturated group, such as the aryl ring, to bond to the palladium.

Keywords: Carbene; DFT; Palladium; Oxidative addition; Mechanism; Arylamination

1. Introduction

The palladium-catalysed amination of aryl halides has become an important method for the synthesis of arylamines found in pharmaceuticals, agrochemicals and new materials [1,2]. The importance of this synthetic method has led to extensive efforts to find catalysts that provide high turnover numbers, reaction rates and functional group compatibility. The initiating step of oxidative addition of the aryl halide to a Pd(0) complex is common to many other important coupling reactions such as Suzuki reactions [3], Heck olefinations [4], and Stille couplings [5]. For the large majority of these studies phosphines are the supporting ligands [6–9]. The nature of the active intermediate depends on the bulk of the phosphine, oxidative addition taking place to a 12 electron Pd centre with bulkier phosphines and to a 14 electron centre with less sterically demanding ones [7–9]. Evidence has also been produced for the active intermediate being an anionic tricoordinated complex such as [PdL$_2$Cl]$^-$ or [PdL$_2$(OAc)]$^-$ [6].

A common procedure when using N-heterocyclic carbenes (NHCs) as supporting ligands for Pd catalysts is to generate the NHC situ from a imidazolium or imidazolinium salt [10]. Palladium *bis*-carbene complexes, [Pd(*cyclo*-C{NRCH}$_2$)$_2$], **1**, have been shown to act as catalyst precursors in aryl amination reactions [11–16]. For example, a palladium N-heterocyclic carbene (NHC) complex useful in the coupling of amines to aryl chlorides (Scheme 1) is [Pd(*cyclo*-C{N^{t}BuCH}$_2$)$_2$] (**1c**).

Complexes such as **1c** can be formed via metal vapour synthesis in which palladium vapour is co-condensed with 1,3-di-*N*-*tert*-butylimidazol-2-ylidene [17]. Alternatively **1c** may be synthesised by the addition of sodium dimethylmalonate to [{Pd(η^3-C$_4$H$_7$)Cl}$_2$] in the presence of two equivalents of 1,3-di-*N*-*tert*-butylimidazol-2-ylidene [13]. Whilst numerous studies have been carried out into the nature of four-coordinate metal(II) carbene species [18], the reactivity of the two-coordinate palladium(0) carbene species is less well documented. Herrmann et al. [19] reported the use

* Corresponding author.
E-mail address: jennifer.green@chem.ox.ac.uk (J.C. Green).

0022-328X/$ - see front matter © 2005 Elsevier B.V. All rights reserved.
doi:10.1016/j.jorganchem.2005.07.117

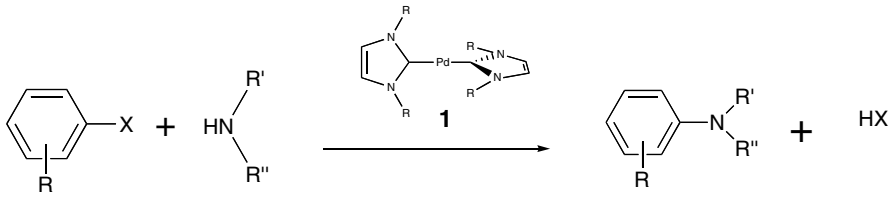

Scheme 1.

of pre-formed two-coordinate palladium(0) NHC complexes such as **1** for Suzuki reactions, noting significant differences in activity compared with complexes generated in situ from a solution containing a mixture of an imidazolium salt (such as the chloride salt of (2,4,6-trimethylphenyl)imidazol-2-ylidene) and $Pd_2(dba)_3$. Nolan and co-workers [2,20] employ $[(NHC)PdCl_2]_2$ as precatalysts for the formation of C–C and C–N bonds, and note that this compound provides the ideal 1:1 ratio of Pd to NHC.

The proposed mechanism for the amination of aryl chlorides by primary, secondary and aryl amines in the presence of **1** is shown in Scheme 2. The reaction pathway is similar to that proposed in analogous palladium phosphine systems. The catalytically active species is proposed to be a mono-carbene complex, **2** [20]. This is supported by experimental studies by Cloke et al. [16] who observed that the optimum ratio of palladium-precursor to imidazolium salt is 1:1. A second equivalent of imidazolium salt impedes the reaction. Kinetic studies support a mechanism for the oxidative addition of *para*-chlorotoluene to complex **1** in which there is a pre-equilibrium step involving dissociation of an NHC ligand from **1** to form **2**.

The electronic structure of the bis-NHC complexes has been examined by photoelectron spectra and density functional calculations of **1c** [21,22]. These studies demonstrated that bonding between the palladium and NHC occurs predominantly through σ-donation from the carbene divalent carbon lone pairs into a Pd $(d_{z^2} + s)$ hybrid, with little evidence of a π back-donation from the transition metal d orbitals to the NHC unfilled out-of-plane π-orbitals. This lack of π back-bonding is anticipated due to significant π-donation into the out-of-plane π-orbitals of the divalent carbon by the nitrogen atoms. Tight binding of the carbenes to the Pd generates an annular ring of electron density around the Pd, formed from the $(d_{z^2} - s)$ HOMO, that inhibits further coordination. Palladium–carbene ligand bond energies are typically very high [22], and the existence of a monoligated palladium complex as the reactive species might appear to be energetically prohibitive.

There have been a number theoretical studies of oxidative addition of aryl halides to Pd complexes. The majority of these involve bis-phosphine palladium catalysts [23–27]. Cundari [28] has recently reported a density functional study based on Buchwald's work [29–31] with very bulky phosphines that compares mono- and bis-phosphine palladium moieties as catalysts [28]. This work also models the reductive elimination step involved in aryl-nitrogen bond formation. Reductive elimination has also been studied

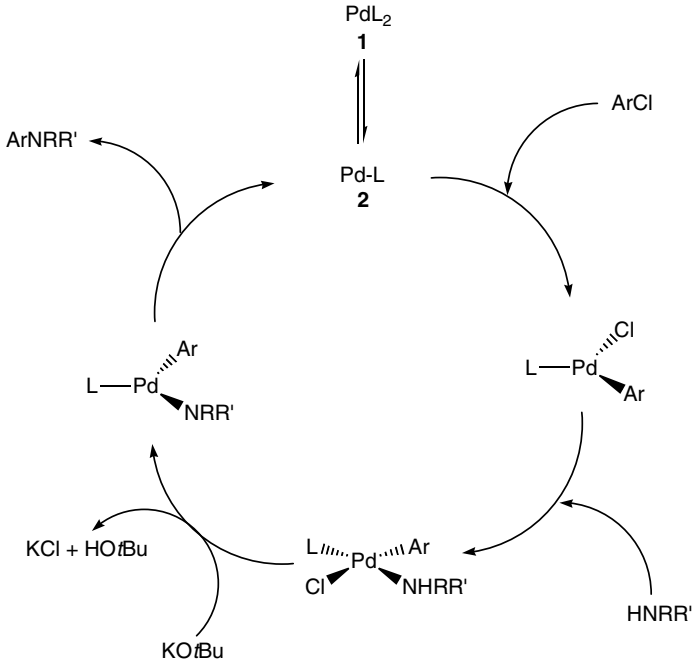

Scheme 2.

for model $M(PH_3)_2(CH_3)(X)$ species ($X = CH_3$, NH_2, OH, and SH) and a comparison made between pathways involving a four-coordinate Pd centre and a three-coordinate one generated by phosphine loss [32]. For palladium NHCs, Rösch reported a study of the Heck reaction using two diaminocarbene ligands [33] to model the bis-NHC palladium catalysts of Herrmann et al. [34].

A number of processes are available for the production of alkyl amines. The most simple of these is nucleophilic substitution of an alkyl halide by ammonia. The yield in this reaction is typically poor since the resulting primary amine is itself a nucleophile and hence products are a mixture of primary, secondary and tertiary amines, as well as tertiary ammonium salts. Other methods of alkyl amine preparation include reduction of amides [35], imides, nitriles [36] or azides; reductive amination reactions [37]; the Hofmann rearrangement [38]; and the Curtius rearrangement [39]. All of these routes are limited by reagents and are therefore not generally applicable. A route analogous to that for aryl halides would be advantageous since the reagents are cheap and readily available and the selectivity for products would be higher. Although the catalytic cycle shown in Scheme 2 is successful experimentally in the amination of aryl halides, there has been no experimental evidence to show that this cycle would work for the amination of alkyl halides.

This paper describes a computational investigation into key steps in this proposed catalytic cycle. Specifically, we address various questions. Solvated species of the *bis*- and *mono*-carbene complexes of Pd are modelled and the oxidative addition step is investigated to determine whether a monoligated palladium complex is the active species. The role of the bulky substituents on the carbene is clarified and the energetics of the reductive elimination of the aryl amine are computed. The oxidative addition of alkyl halides is also explored and crucial differences from aryl halides are identified.

2. Computational methods

Calculations were performed using GAUSSIAN 03, rev. A2 [40]. The exchange-correlation functional used was BP86 [41–43]. Two basis set combinations were employed. Basis set I used a SDD ECP basis set for palladium with a small core [44,45], and the split valence 6-31G** for all other atoms [46–51]. Basis set II used a SDD basis set for palladium [44,45], with the cc-pVDZ basis sets of Dunning et al. [52–54] for all other atoms. Basis set I was used for geometry optimisations, solvent effects and frequency calculations. Basis set II was used for improved accuracy single point calculations. The calculation of solvent effects employed the PCM model [55–58], using the default radii of the program. The solvent used was benzene ($\varepsilon = 2.284$).

Reaction energetics, given in the tables, were calculated for various levels. Initially the differences in energy of the geometry optimised structures were calculated, then this number was further refined by using the more accurate basis sets in single point calculations. Zero-point energy corrections were added to give an estimate of ΔU^0 at 0 K. The frequency calculations were then used to obtain a gas phase Gibbs free energy change at 298.15 K, ΔG^0_{298}. Finally solvent corrections were made to this Gibbs free energy.

One problem with the methodology being applied is the calculated entropy terms refer to the gas phase entropy. Depending upon the size of the molecules, the entropy term has between 30–60% translational and rotational contribution. Smaller molecules have fewer vibrational normal modes, therefore proportionally have a larger contribution from translational and rotational entropy. In solution, these terms will be reduced, as molecular tumbling and translation are hindered by solvent–solute interactions. The data given in the tables therefore represents an overestimate of the reaction free energies for associative reactions (i.e., are too positive), and an underestimate for dissociative reactions (i.e., are too negative).

3. Results and discussion

3.1. General approach

Studies of reaction pathways should in principle be carried out on a Gibbs free energy surface as a function of temperature. This is not currently possible and normal practice is to compute reaction pathways on an SCF energy surface to identify minima, as models for intermediates, and saddle points, as models for transition states. The Gibbs free energies of these structures are then computed to give estimates of reaction energetics and activation energies. The benefit of this approach is that it illuminates crucial electronic factors that control reactivity.

Chemical intuition would suggest that the steric bulk of the *tert*-butyl groups in complex **1c** prevents an associative mechanism, whereas oxidative addition by such a mechanism to **1a** might well be possible. A key goal of this study was to determine whether steric factors are important in determining the reactivity. Therefore, the ligand set **a**–**c** shown below was chosen to investigate the oxidative addition mechanism.

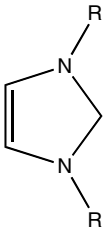

a, R = H
b, R = Methyl
c, R = *tert*-Butyl

3.2. Structures

The structures of the bis-carbene complexes were optimised without symmetry constraints to give the D_{2d} symmetry structures shown in Fig. 1. The palladium–carbon bond lengths for **1a**–**c** are in good agreement with those ob-

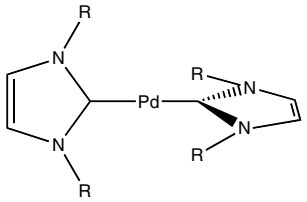

	Pd-C
1a, R = H	2.001
1b, R = Methyl	2.018
1c, R = *tert*-Butyl	2.061

Fig. 1. Structure of complex **1a–c**. Pd–C bond length is given in Å.

tained in a previous study using the BP86 functional and Slater type orbitals [22].

The structures of the mono-carbene complexes **2a–c** were optimised without symmetry constraints to give the structures shown in Fig. 2. The palladium–carbon bond lengths are circa 0.09 Å shorter than the bis carbene complexes for ligands **a** and **b**, and circa 0.11 Å shorter for the bulkier ligand **c**.

Steric effects are expected to be small in complex **2**, as the alkyl groups are not interacting with the opposite carbene ligand. Therefore, the palladium–carbon bond length should be a reflection in the energetics of the bonding of the NHC to palladium.

3.3. Ligand dissociation energies of the bis-carbene complexes

Energetics for the dissociation reaction (1) for complexes **1a–c** are given in Table 1. There is a clear trend that the bulkier the ligand substituent groups, the lower the dissociation energy of the bis-carbene complex. The entropy term gives the largest correction to the energy of dissociation, as would be expected for a dissociative reaction. The solvent corrected energy barriers are in the range to be accessible at moderate temperatures. Thus, despite the high bond enthalpy, it is possible for small amounts of mono substituted palladium carbene complexes to be generated in solution at the temperatures typically used for the amination reactions [59]. It is also the case that any adventitious hydrogen ions may protonate the dissociated carbene and assist formation of catalytic amounts of the mono-carbene complex.

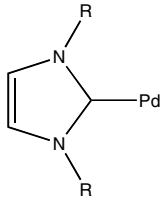

	Pd-C
2a, R = H	1.909
2b, R = Methyl	1.927
2c, R = *tert*-Butyl	1.955

Fig. 2. Structure of complex **2a–c**. Pd–C bond length is given in Å.

Table 1
Energies for the dissociation reaction (1) for complexes **1a–c**

Complex	GGA energy	Larger basis set	ZPE corrected	Free energy	Solvent corrected
1a	225.8	213.6	208.2	157.4	159.1
1b	225.6	202.6	197.5	140.0	135.0
1c	194.0	185.5	180.2	111.8	119.4

Values shown are in kJ mol^{-1}, and are calculated at 298.15 K in benzene. Details of the corrections can be found in Section 2.

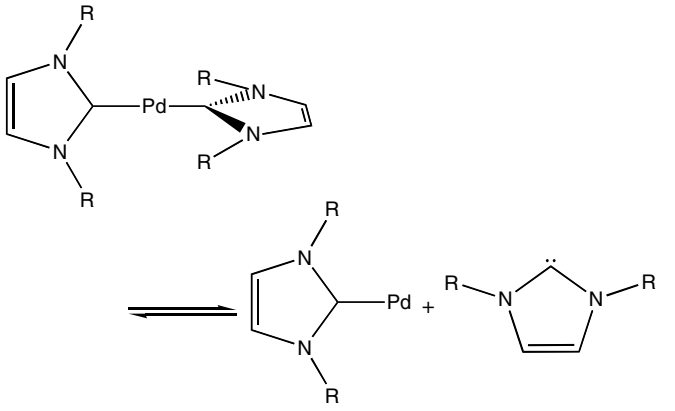

(1)

3.4. Palladium–carbene–solvent complexes

The energy associated with dissociation of a ligand to form a mono-carbene palladium complex does not prevent this from occurring as part of a chemical reaction. However, most amination reactions are performed in benzene or other similar solvent [16]. Therefore, it is likely that specific solvent palladium interactions will occur that greatly stabilise the monosubstituted complex formed. The structure and energetics of various palladium–carbene–solvent complexes that may form when complexes **1a–c** are dissolved in benzene were examined.

3.5. Structures

The mono substituted complexes **2a–c** were optimised with a benzene ligand coordinated to the palladium metal, to give an η^2 structure, **3a–c**, shown in Fig. 3. The Pd–carbene C bond lengths (parameter α in Fig. 3) are substantially longer than in the mono substituted complexes, and approach those of the bis-carbene complexes **1a–c** given in Fig. 1.

A second benzene ligand was added to complexes **3a–c** and optimised to give the structures, **4a–c** shown in Fig. 4. The palladium–carbene distances are longer in complexes **4a–c** than in **1a–c**. The less sterically demanding ligands have shorter Pd–benzene distances, a reverse of the

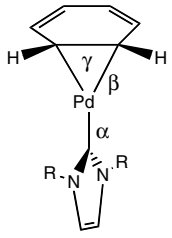

	α	β	γ
3a, R = H	1.996	2.234	1.429
3b, R = Methyl	2.016	2.230	1.430
3c, R = *tert*-Butyl	2.053	2.228	1.430

Fig. 3. Structure of the η^2-benzene palladium carbene complexes **3a–c**. Parameters α, β and γ are given in Å. β represents the average of Pd–C distances to the two coordinating benzene carbon atoms.

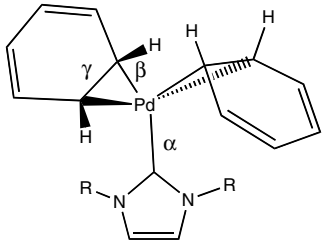

	α	β	γ
4a, R = H	2.062	2.284	1.439
4b, R = Methyl	2.072	2.309	1.435
4c, R = *tert*-Butyl	2.115	2.352	1.432

Fig. 4. Structure of the bis η^2-benzene palladium carbene complexes **4a**–**c**. Parameters α, β and γ are given in Å. β represents the average of Pd–C distances to the two coordinating benzene carbon atoms, and γ the average coordinated carbon–carbon distance in the two benzene rings.

trend in the mono solvent complexes **3a**–**c**. This suggests that steric crowding is probably becoming a more dominant factor in complexes **4a**–**c**.

A benzene molecule was added to the bis-carbene palladium complexes **1a**–**c**, and the resultant structures optimised to give the structures, **5a**, and **5b** shown in Fig. 5.

The *tert*-butyl groups of ligand **c** prevented a stable adduct forming, and the benzene molecule preferentially decoordinated. The palladium–carbene carbon distances are longer than in the bis-carbene complexes, and are comparable to those in the three-coordinate complexes **4a** and **4b**. The importance of steric effects reducing palladium solvent interactions for the bis-carbene complexes is supported by the lack of bis-carbene palladium benzene complex for ligand **c**.

3.6. Energetics

The energetics for the reactions (2)–(6) are shown in Table 2. In general, when two molecules combine to form a complex, the free energy of activation is substantially higher than the zero-point energy differences. This is a reflection of the reduction of entropy of the system. Thus, reactions (2), (4) and (6) are unfavourable. The reverse is true of a complex that dissociates into two molecules. Hence reaction (5) is actually favourable when R = Me.

Solvent association to the bis-carbene complex (reaction (2)) becomes less favourable with increasing ligand bulk. This extends to the observation that the very bulky *tert*-butyl carbene ligand does not form a bis-carbene solvent complex. The steric crowding that is present in the ground state bis-carbene complexes is reduced on forming a mono-carbene solvent complex. Formation of a bis-solvent carbene complex is not favourable. Both reactions (4) and (6) are uphill, and not only due to the loss of entropy term.

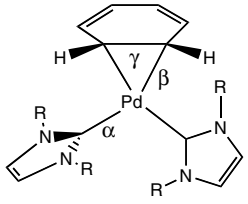

	α	β	γ
5a, R = H	2.054	2.244	1.451
5b, R = Methyl	2.070	2.275	1.446

Fig. 5. Structure of the bis carbene η^2-benzene palladium carbene complexes **5a** and **5b**. Parameters α, β and γ are given in Å. β represents the average of Pd–C distances to the two coordinating benzene carbon atoms.

Table 2
Energies for the solvent association reactions (2)–(6) for complexes **1a**–**c**

Reaction complex	GGA energy	Larger basis set	ZPE corrected	Free energy	Solvent corrected
(2)					
1a	28.6	32.2	29.6	79.5	85.0
1b	38.8	35.3	32.4	80.1	75.5
(3)					
1a	126.7	118.6	113.9	109.9	111.8
1b	125.6	108.4	103.6	70.2	69.4
1c	93.3	89.8	85.2	64.4	76.6
(4)					
1a	131.1	127.3	122.7	175.4	178.5
1b	138.5	123.6	119.3	165.6	161.7
1c	133.1	132.3	129.7	168.7	172.7
(5)					
5a	98.1	86.4	84.3	30.4	26.7
5b	86.8	73.0	71.2	−9.8	−6.1
(6)					
3a	4.4	8.7	8.7	65.5	67.7
3b	12.9	15.2	15.7	95.4	92.3
3c	38.9	42.5	44.6	104.3	96.1

Values shown are in kJ mol^{-1}, and are calculated at 298.15 K in benzene. Details of the corrections can be found in Section 2.

The choice of ligand system used to model the reactions appears reasonable. The ligands a, b and c reflect a broad range of reactivity, and it is clear there is a change over in some of the above equilibriums when changing to the bulky ligand c. The extra computational cost required to treat the large alkyl groups correctly is rewarded by revealing the true reactivity of the real system.

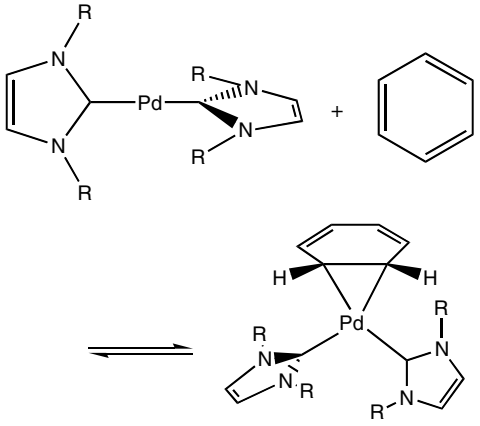

(2)

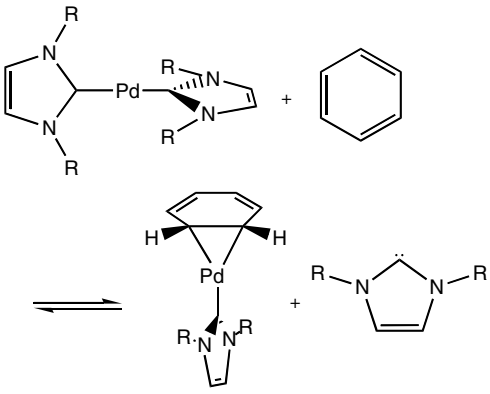

(3)

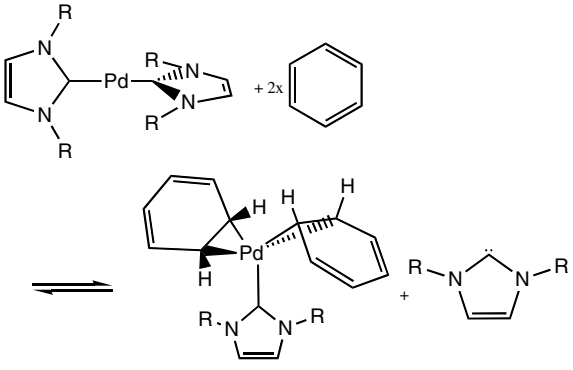

(4)

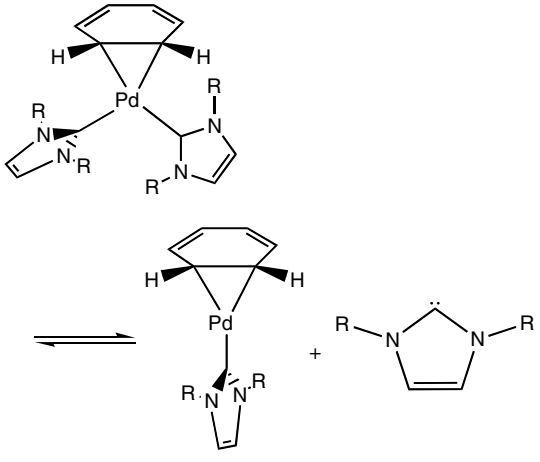

(5)

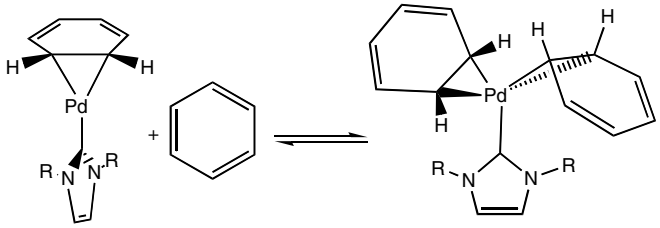

(6)

3.7. Oxidative addition transition states

The solvent complexes detailed above were investigated to determine whether they allowed oxidative addition of chlorobenzene. Initially, the solvent complexes were optimised with one chlorobenzene replacing a benzene ligand. The structures obtained are of similar energy (to within 10 kJ mol^{-1}) to the benzene complexes, and act as the reference level for the oxidative addition transition state energies detailed below.

The transition state, **6a**–**c**, for oxidative addition in complexes **3a**–**c** is shown in Fig. 6 below.

To verify that **6a** is the correct transition state for oxidative addition, an intrinsic reaction coordinate (IRC) calculation was allowed to progress from the transition state to the minima it connects. One direction led easily to **3a**, the solvated mono-carbene palladium complex. The other direction leads to a T-shaped palladium carbene phenyl chloride complex, **7a**, the correct oxidative addition product, as shown in Fig. 7. As a comparison for the data given in Fig. 6, the bond lengths in the optimised oxidative addition product are ~2.34 Å for the Pd–Cl bond, and ~1.98 Å for the Pd–Ph bond.

Geometry optimisations were carried out on three possible isomers of the oxidative addition product when

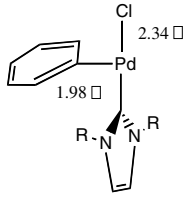

7a

Fig. 7. T-shaped oxidative addition product, **7a**, R = H.

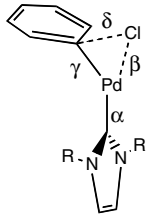

	α	β	γ	δ	ν / cm^{-1}
6a, R = H	2.044	2.460	2.024	2.142	161i
6b, R = Methyl	2.058	2.469	2.029	2.121	161i
6c, R = *tert*-Butyl	2.085	2.508	2.029	2.104	159i

Fig. 6. Structure of the oxidative addition transition states **6a**–**c**. Parameters α, β, γ and δ are given in Å. ν is the frequency of the imaginary mode corresponding to motion over the transition state.

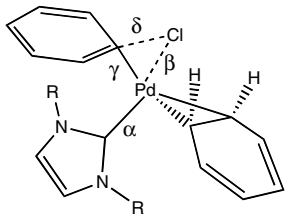

	α	β	γ	δ	ν /cm^{-1}
8a, R = H	2.043	2.627	2.184	1.945	128i
8b, R = Methyl	2.056	2.618	2.122	2.064	175i

Fig. 8. Structure of the oxidative addition transition states **8a** and **8b**. Parameters α, β, γ and δ are given in Å. ν is the frequency of the imaginary mode corresponding to motion over the transition state.

R = Bu^t. The structure in which the carbene is trans to the chloride ligand (as shown in Fig. 7) was found to be 39 kJ mol^{-1} lower in energy compared to the conformer in which the phenyl ring is trans to the carbene ligand, Attempts to optimise the structure with the phenyl group trans to chlorine resulted in the more stable configuration shown in Fig. 7.

Parameters β and δ in Fig. 6 suggest the transition state is slightly earlier for the bulkier ligand **c**. This is in agreement with the data for the ground state solvent complexes **3** shown in Fig. 3. Thus bulkier ligands have shorter metal solvent bonds in the ground state, and an earlier oxidative addition transition state, in the mono solvated complexes.

The transition state (**8a** and **8b**) for oxidative addition to complexes **4a**–**c** is shown in Fig. 8.

Again, the transition state was verified as correct by an IRC calculation on **8a**, with one direction progressing to complex **4a** and the other to an oxidative addition product. A transition state could not be found for the *tert*-butyl complex. In attempted optimisations of **8c**, the spectator solvent molecule decoordinated from the palladium, and the resultant complex optimised to **6c**. As a comparison for the data given in Fig. 7, the bond lengths in the optimised solvated oxidative addition product are ~2.45 Å for the Pd–Cl bond, and ~2.02 Å for the Pd–Ph bond.

The data given in Fig. 8 shows a reasonably clear trend. As the ligand becomes more bulky, the oxidative addition transition state occurs later on the reaction surface, with longer parameters β and δ, and a shorter parameter γ. This is in agreement with the data for complex **4** shown in Fig. 4, where the bulkier ligands have longer metal solvent bond lengths. The formation of the more crowded oxidative addition transition state is disfavoured by an increase in steric bulk of the ligands. Thus for the *tert*-butyl substituted ligand, formation of **7c** is not possible, and the spectator benzene ligand is preferentially decoordinated.

Numerous transition state optimisations were attempted on complex **5a** to find a transition state for oxidative addition. In several of these, the chlorine atom was lost, and did not form a bond to the metal centre. A structure that consistently occurred during attempted optimisations has C_S symmetry, with the chlorine atom H-bonding to the hydrogens of the carbene ligands, as shown in Fig. 9.

The frequency calculation on complex **9a** had an imaginary mode at 130i cm^{-1} corresponding to the chlorine atom moving away from the phenyl ring. An IRC calculation did not progress to an oxidative addition product. Instead, the chlorine atom moved further from the phenyl ring to H-bond to the carbene ligands.

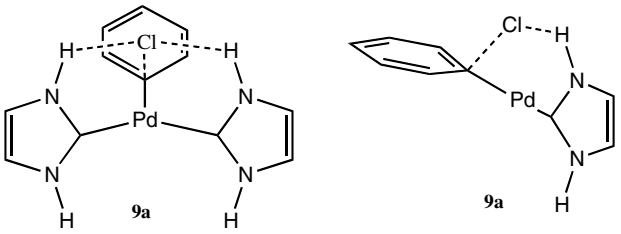

Fig. 9. C_S symmetry structure obtained while optimising for an oxidative addition transition state in complex **5a**. The chlorine atom is H-bonded to both carbene ligands. An imaginary normal mode and 110i cm^{-1} corresponds to the chlorine atom moving away from the phenyl ring.

Complex **9a** clearly does not correspond to an oxidative addition transition state. Instead, it corresponds to chloride being lost to H-bond between the carbene ligands. To avoid the strong H-bonding from the hydrogen substituents in ligand **a**, ligand **b** was used in an attempt to optimise an oxidative addition transition state in complex **5b**. All attempts converged to an analogous transition state to **9a**. This suggests that the metal centre is not electrophilic enough to oxidatively add an aryl chloride in the linear bis-carbene complexes. The annular ring of electron density repels the reactant.

3.8. Energetics of oxidative addition

The activation energetics of reactions (7)–(10) are shown in Table 3. Initially considering the oxidative addition from the chlorobenzene complexes, the data for reactions (7) and (8) show that as the steric bulk of the carbene ligand increases, the oxidative addition becomes easier in the mono solvent complex, and harder in the bis solvent complex. From the trends discussed above, this is consistent with the early transition states having lower activation energies.

The data for reactions (9) and (10) represent the reaction energies for oxidative addition of chlorobenzene to the bis carbene palladium complexes. A comparison between (9) and (10) for ligand **a** shows that complex **1a** has very similar zero-point activation energy barrier for the two transition states **6a** and **8a**. Changing the ligands to larger substituents results in the mono solvent oxidative addition transition states **6b**–**c** having lower zero-point activation energies.

Table 3
Energies for the formation of the oxidative addition transition state, as shown in reactions (7)–(10) for complexes **1a**–**c**

NHC	GGA energy	Larger basis set	ZPE corrected	Free energy	Solvent corrected
(7)					
a	45.9	44.3	42.3	40.5	41.4
b	46.1	44.5	42.3	38.4	39.4
c	41.8	41.4	40.2	32.2	–
(8)					
a	32.5	31.9	30.2	25.4	26.0
b	38.7	38.0	37.0	37.4	41.2
(9)					
a	179.4	167.6	159.9	152.8	157.3
b	176.9	154.9	147.3	134.8	137.0
c	140.8	132.2	126.1	106.3	–
(10)					
a	170.9	164.8	157.4	207.8	215.1
b	186.1	168.7	162.2	206.3	208.7

Values shown are in kJ mol^{-1}, and are calculated at 298.15 K in benzene. Details of the corrections can be found in Section 2. A solvent calculation was not possible on complex **7c**, due to problems constructing a suitable cavity.

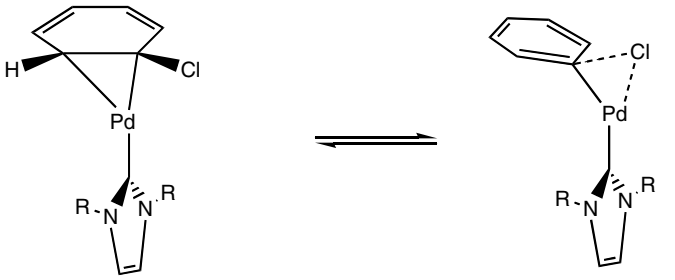

(7)

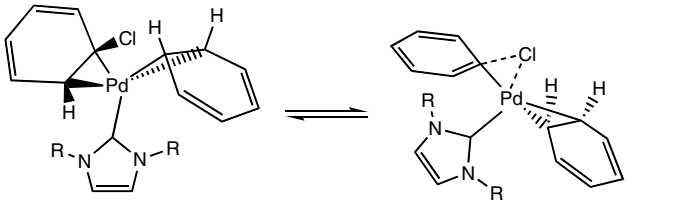

(8)

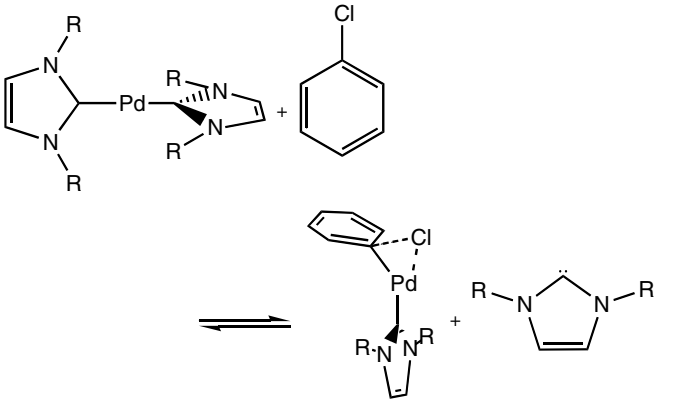

(9)

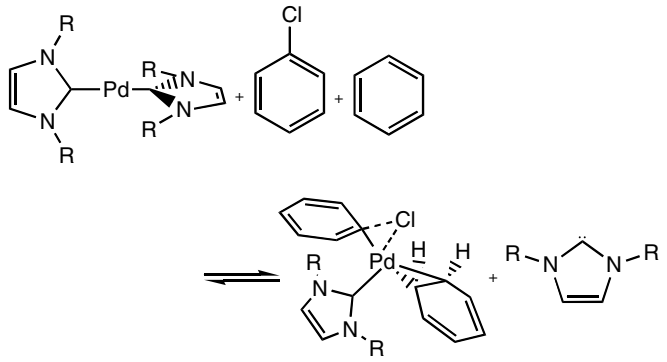

(10)

Formation of the bis solvent oxidative addition transition state, in free energy terms, is greatly disfavoured, due to the loss of entropy from coordinating an additional solvent molecule. Hence, the rate determining transition state for oxidative addition in all complexes is likely to be **6**. The reaction energy of (9) is substantially lower for ligand **c** than **a** or **b**. Comparison of the data in Tables 2 and 3 show that the largest contributor to this difference is the more favourable dissociation of the bulky carbene ligands, as given in reaction (1).

Subsequent steps in the catalytic cycle were studied only for the bulky ligand **c** as this gave the most realistic comparison with experiment.

3.8.1. Bis-carbene palladium aryl halide

In the absence of aryl amine the product of oxidative addition of an aryl halide is *trans*- [Pd(*cyclo*-C{N^{t}BuCH}$_2$)$_2$-(Cl)(Ph)] [15]. Coordination of a carbene to the more stable intermediate shown in Fig. 7 would suggest formation of the *cis* isomer. Therefore the bis-carbene oxidative addition product [Pd(*cyclo*-C{N^{t}BuCH}$_2$)$_2$(Cl)(Ph)] **10c** was also investigated. The optimised structure and selected parameters are shown in Fig. 10. The *trans*-isomer was found to be lower in energy than the *cis*-isomer by 71 kJ mol^{-1} as it reduces the steric interactions between the bulky *t*-butyl substituents on the carbene. Experimental bond lengths and angles for [Pd(*cyclo*-C{N^{t}BuCH}$_2$)$_2$(CO$_2$Me-4-C$_6$H$_4$)(Cl)] (**10c′**) are provided in Fig. 10 for comparison.

3.8.2. Binding of aniline to intermediate 7c

Consequent to determination of the lowest energy structure for intermediate **7c**, the product, **11c**, of the coordination of aniline to **7c** was investigated. Geometry optimisations were performed on the possible stereoisomers of complex **11c**. The isomer with the phenyl ring trans to the chlorine ligand was found to be lowest in energy (Fig. 11). The most significant difference in bond vectors between **10c** and **11c** is the Pd–C(NHC) distance which is ~0.11 Å shorter. This is a consequence of the increased trans influence of carbene compared with aniline, a reflection of the superior σ-donating capabilities of carbenes. The *cis*-arrangement of the amine and the aryl group is favourable for subsequent reductive elimination after removal of HCl.

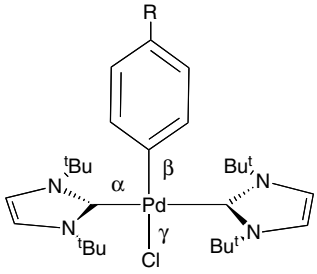

		α	β	γ
10c	R = H	2.111	2.065	2.477
10c'	R=CO_2Me	2.091	2.060	2.428

Fig. 10. Comparison of experimental [15] and calculated structures of [Pd(NHC)$_2$(C_6H_4R)Cl]. Parameters α, β, and γ are given in Å.

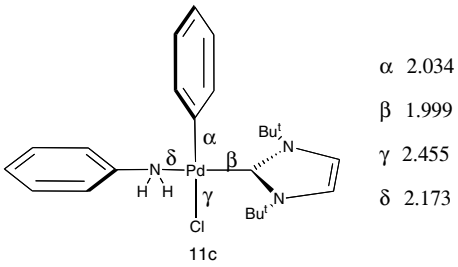

α 2.034
β 1.999
γ 2.455
δ 2.173

11c

Fig. 11. Optimised geometry of **11c**. Parameters α, β, γ and δ are given in Å.

The energetics found so far for the tertiary butyl NHC Pd system are summarised in Fig. 12.

3.8.3. Palladium-amido intermediate

The step involving the removal of H^+ and Cl^- from **11c** by potassium *t*-butoxide was not studied in detail since the thermodynamic driving force is the formation of KCl and HOBu^t. The product of this step, **12c**, is shown in Fig. 13. Akin to **7c**, this complex displays a T-shaped geometry. The Pd–N bond is significantly shorter in this complex than in **11c** (0.16 Å shorter) and lies in the range expected for palladium-amido species. The concomitant loss of H^+ with formation of an amido-bond results in the palladium-centre in **12c** retaining a 16 electron count. The Pd–carbene bond length is increased in comparison to **11c** (by 0.04 Å) due to the increased trans influence of an amide compared with an amine.

3.8.4. Reductive elimination of ArNRH from complex *13c*

The final step of the catalytic cycle is the reductive elimination of diphenylamine from complex **13c**. A transition state for reductive elimination, **14c** (Fig. 14) was found.

The optimised transition state displays a single imaginary frequency indicating a negative force constant. To

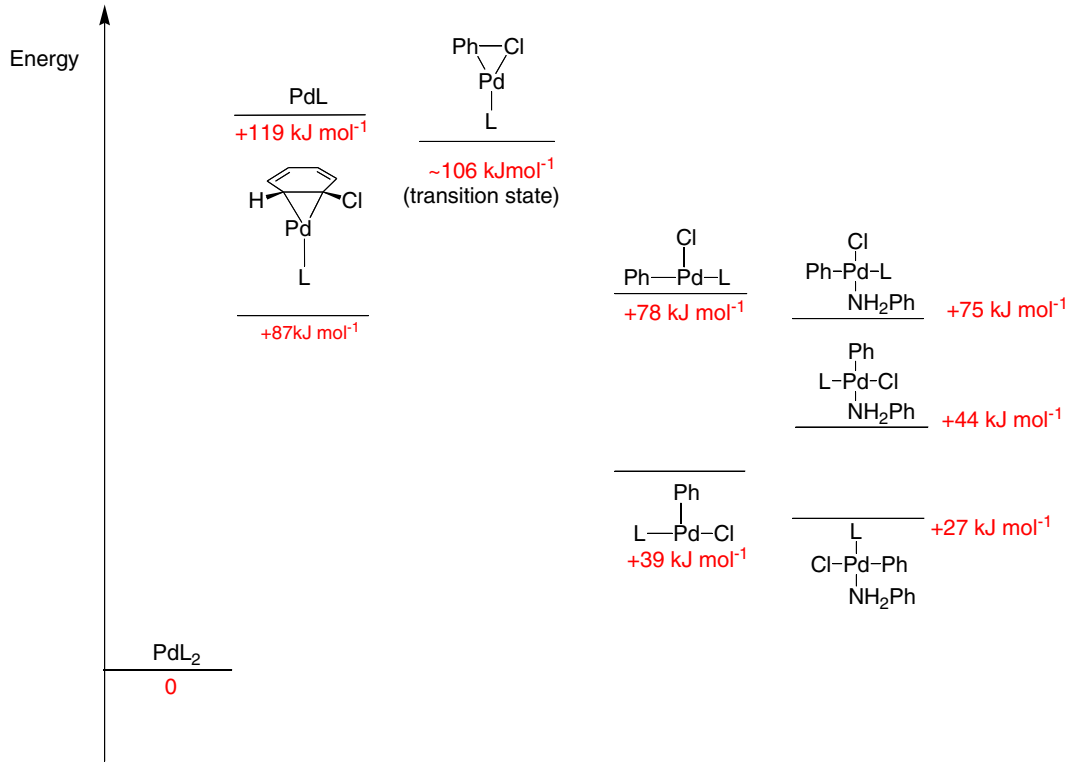

Fig. 12. Relative free energies of oxidative addition and insertion products. L = cyclo-C{N^{t}BuCH}. (The energy given for the transition state is the gas phase value as the solvent correction failed.)

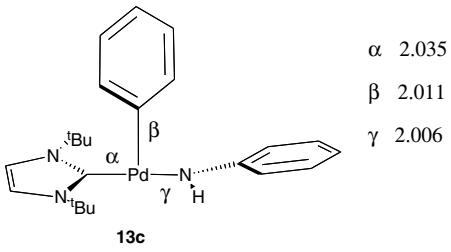

Fig. 13. Optimised geometry of **13c**. Parameters α, β , and γ are given in Å.

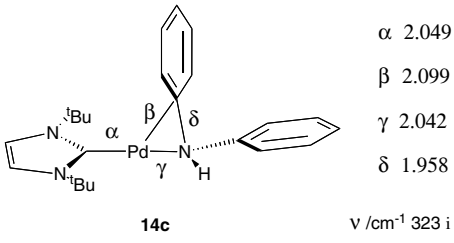

Fig. 14. Transition state for reductive elimination of diphenylamine. Parameters α, β, γ and δ are given in Å. ν is the frequency of the imaginary mode corresponding to motion over the transition state.

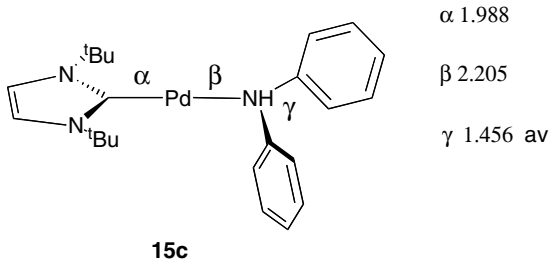

Fig. 15. Intermediate formed on reductive elimination of diphenylamine. Parameters α, β and γ are given in Å.

verify that this was the correct transition state for reductive elimination, the IRC was investigated around this point. The local minimum in one direction was **13c**. In the other direction the structure evolved to diphenylamine coordinated to the mono-carbene Pd (**15c**) shown in Fig. 15, thus confirming that structure **14c** is indeed a transition state for reductive elimination. The N retained its trans configuration with respect to the carbene throughout the elimination.

The Pd–N bond length in **15c** is 2.205 Å (compared to 2.006 Å in **13c**) as a result of the nitrogen becoming coordinatively saturated.

By analogy with the coordination of chlorobenzene to the Pd centre, as represented by structure **3c**, a structure was postulated in which the palladium is bonded in an η^2 fashion to the phenyl ring of diphenylamine. Though the starting structure had the Pd coordinated to the C(1)–C(2) bond of the phenyl ring immediately adjacent to the N, the optimised structure, **16c**, had the Pd coordinated to the C(2)–C(3) bond (Fig. 16). The mesomeric effect of the N would be expected to maximise electron density in

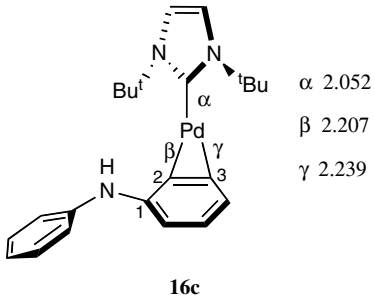

Fig. 16. Structure of η^2 coordinated diphenylamine. Parameters α, β and γ are given in Å.

this location. The free energy of **16c** (inclusive of solvent effects) was calculated to be lower than that of **15c** by 44 kJ mol^{-1}.

The energy profile for reductive elimination from **13c** resulting in the more stable **16c** is shown in Fig. 17. A detailed breakdown of the relative energies are given in Table 4. The free energy barrier to reductive elimination was calculated to be 64 kJ mol^{-1}.

Replacement of the amine by a further molecule of aryl chloride would release the aryl amine product and recommence the catalytic cycle.

3.9. Comparison with previous studies

Previous computational studies employing bis-ligated palladium have found similar η^2-arene complexes and oxidative addition transition states to those reported here [23,25–27]. The most directly comparable study is that of Cundari and Deng [28] who model the catalytic cycle for $Pd(PH_3)$ and $Pd(PH_3)_2$. They argue that the monophosphine compound is the more active catalyst because it lowers the barriers to oxidative addition and reductive elimination compared with the bisphophine complex. Our findings are similar. In addition we find that the bulky tertiary butyl NHC lowers the energy of ligand dissociation needed for formation of the monocarbene complex. They report arene η^1 coordination being the most stable whereas we find an η^2 complex. The most stable isomer for the oxidative addition product is with the phosphine trans to the halide as found for the oxidative addition product **7** described here with the carbene trans to the chloride. Also the most stable isomers of the analogues of **11c** and **13c** have the same stereochemistry as those we describe. The energetics of the two studies are not strictly comparable in that Cundari and Deng use PhBr as the aryl halide and NH_3 as the amine, but the magnitudes found are not dissimilar. However, they do not report any coordination of the aryl amine formed on reductive elimination comparable to **15c** and **16c**. Macgregor et al. [32], who have studied reductive elimination of CH_3NH_2 from $M(PH_3)_2(CH_3)NH_2$, identified a pathway for reductive elimination from a three-coordinate species formed after phosphine loss, the product of which was a $Pd(PH_3)(NH_2Me)$ with a coordinated

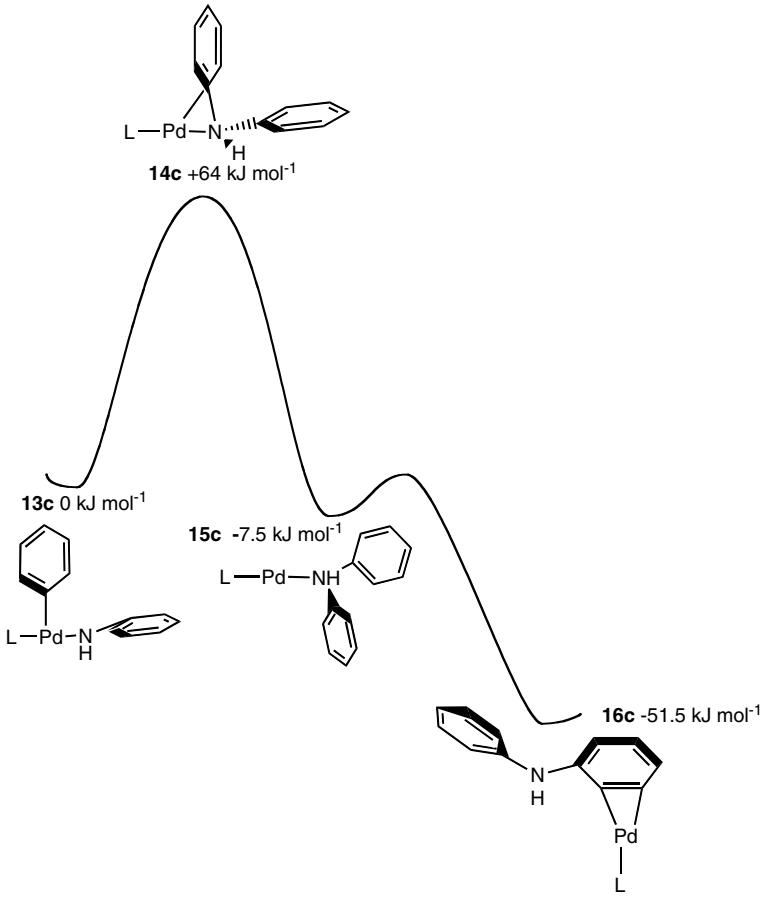

Fig. 17. Free energy profile (inclusive of solvation) for the reductive elimination of aryl amine.

Table 4
Energies of the complexes **14c**, **15c** and **16c** relative to complex **13c**

Reaction complex	GGA energy	Larger basis set	ZPE corrected	Free energy	Solvent corrected
14c	61.2	59.4	56.4	62.3	64.4
15c	−31.3	−29.4	−25.9	−18.5	−7.5
16c	−55.5	−51.2	−49.8	−45.6	−41.2

Values shown are in kJ mol^{-1}, and are calculated at 298.15 K in benzene. Details of the corrections can be found in Section 2.

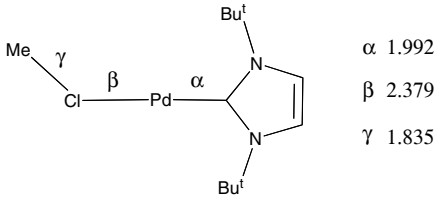

17c

Fig. 18. Monocarbene palladium complex solvated with methyl chloride. Parameters α, β and γ are given in Å.

amine. Their study though lacks an arene in the amine product so there is no competition with coordination to the arene ring, which we identify as a more stable intermediate.

3.10. Oxidative addition of alkyl chlorides

One might postulate that the energy barrier to oxidative addition of alkyl halides is greater than that of aryl halides due to the absence of a phenyl π-system (present in aryl halides) which promotes formation of a solvated complex. The validity of this theory has been investigated by modelling the oxidative addition of chloromethane to complex **2c**.

A local minimum was found corresponding a solvated chloromethane–palladium–NHC complex (**17c**) shown in Fig. 18. Intermediate **17c** is analogous to the solvated chlorobenzene species, **3c**, shown in Fig. 3.

The transition state, **18c**, found for oxidative addition of methyl chloride is shown in Fig. 19. A frequency calculation revealed a single imaginary mode of vibration corresponding to the methyl group moving from the palladium metal to the chlorine atom. The distance between the methyl carbon atom and the chlorine in **18c** is 2.143 Å (compared to 1.805 Å in free chloromethane).

The geometry of **18c** can be rationalised by inspection of Fig. 20 which shows the total electron density of **2c** with the potential superimposed. This shows a region of high positive charge to be located on the palladium metal pointing away from the carbene. It therefore follows that

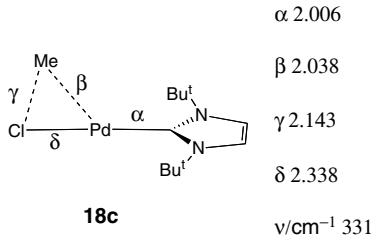

Fig. 19. Transition state for the oxidative addition of methyl chloride to [Pd(NHC)]. Parameters α, β, γ and δ are given in Å. ν is the frequency of the imaginary mode corresponding to motion over the transition state.

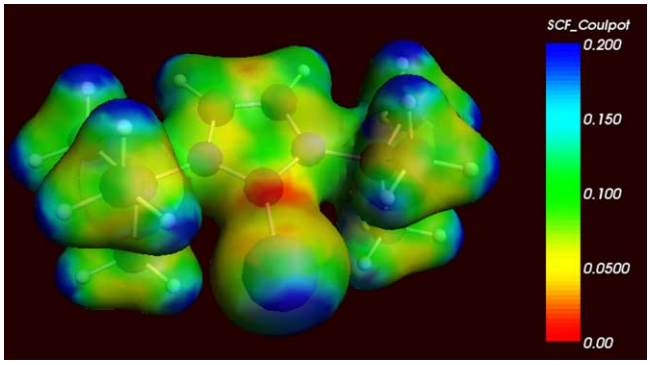

Fig. 20. Total electron density of **2c** with superimposed potential.

the chlorine atom of the chloromethane (which bears a negative charge due to electronegativity effects) should align with the least electron rich part of the palladium metal reducing electrostatic repulsion. The carbon atom of chloromethane is aligned with the more electron rich side of the palladium since it carries a positive charge.

An analogous oxidative addition product **19c** to that of the aryl halides was optimised to the structure shown in Fig. 21. Complex **19c** is 58 kJ mol^{-1} lower in energy than the conformer in which the carbene is trans to the methyl group. Attempts to optimise a structure in which the chlorine is trans to the methyl group were unsuccessful, the structure reverting to the lower energy isomer. The Pd–NHC bond in **19c** is 0.14 Å longer than that of the analogous phenyl complex **10c**. This is a consequence of the stronger σ-donating capability of the methyl group increasing the electron density at the palladium centre.

To verify that complex **18c** is a transition state for the oxidative addition of chloromethane to **2c**, the IRC around **18c**

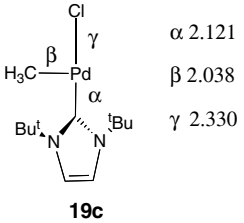

Fig. 21. Optimised geometry of product of oxidative addition of MeCl to the Pd mono carbene complex. Parameters α, β and γ are given in Å.

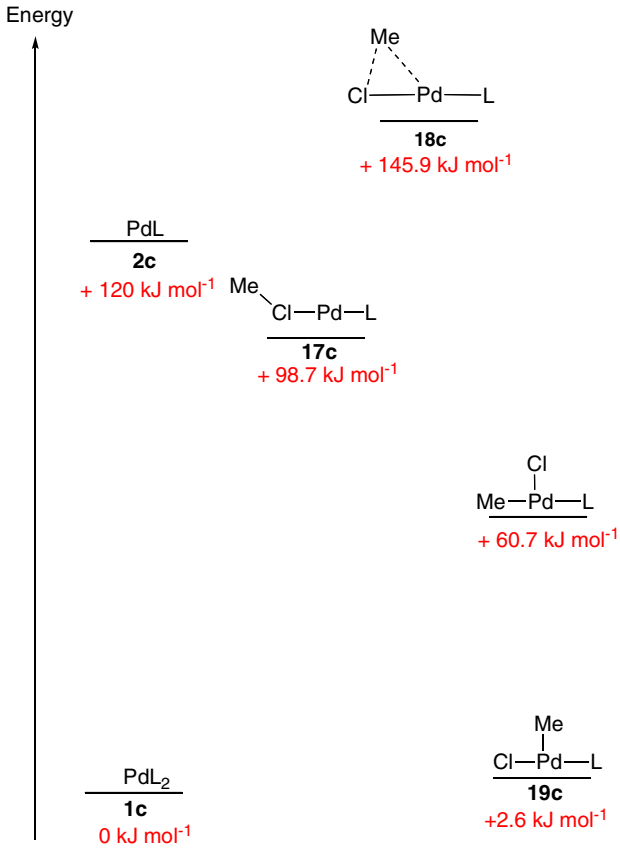

Fig. 22. Energetics for the oxidative addition of methyl chloride to **2c**.

was investigated. The local minimum in one direction was **17c** and **19c** in the other direction thus confirming that complex **18c** is indeed a transition state for oxidative addition.

An energy profile for the oxidative addition of chloromethane to **1c** is shown in Fig. 22. The energy of the transition state **18c** is 47.2 kJ mol^{-1} higher in energy than the intermediate **17c**. In the analogous oxidative addition of chlorobenzene the transition state is higher in energy with respect to the solvated species by around 30 kJ mol^{-1}. An η^2-benzene mono-NHC complex (Fig. 3) has a relative free energy of 86.8 kJ mol^{-1} with respect to **1c** and hence benzene will bind competitively against chloromethane to form **3c**. Should the reaction be performed in the presence of a non-competitive solvent (such as pentane), formation of **2c** would still be preferred over the oxidative addition transition state **18c**.

This leads to the conclusion that oxidative addition of chloromethane to complex **1c** is kinetically unfavourable.

4. Conclusions

The equilibria that may occur when various bis N-heterocyclic carbene palladium complexes are dissolved in benzene were investigated. It was shown that benzene was able to coordinate to the bis carbene complexes when the N–R substituent was H or CH_3. However as the carbene's N-substituent groups became larger, this associative equilibrium was less favourable. In the case of *tert*-butyl

substituted carbene ligands, a bis carbene solvent complex was not stable.

Dissociation of a carbene ligand was calculated to be energetically demanding. However the coordination of a benzene ligand partially compensated for the loss of bonding to the carbene. Coordination of a second solvent molecule to this complex was moderately endothermic on the zero-point energy surface. However, inclusion of entropy terms made formation of the bis-solvent carbene palladium complex highly unfavourable on a free energy surface.

The oxidative addition of chlorobenzene to the palladium carbene complexes was investigated. It was found that the most favourable oxidative transition state was the mono-carbene-aryl chloride palladium complex. Oxidative addition of chlorobenzene to a complex with a spectator benzene ligand also coordinated to the palladium atom was much higher in energy due to the loss of entropy associated with coordinating the second solvent molecule. This bis-solvent oxidative addition transition state was determined to have a favourable zero-point activation energy with sterically minimal carbene ligands. However, the steric crowing in complexes with carbene ligands with larger substituent groups results in higher zero-point activation energies than the mono-solvated complex for oxidative addition. A transition state for oxidative addition to the bis-carbene solvent palladium complex was not found. It is thought the palladium centre is too electron rich to undergo oxidative addition. This supports the proposed dissociative mechanism for oxidative addition.

The amination of chlorobenzene by aniline has been investigated using the mono-carbene solvent complex as a catalyst. Coordination of aniline to the T-shaped oxidative addition product occurs with a rearrangement in configuration placing the amine cis to the aryl group which is necessary for subsequent steps in the catalytic cycle.

The product of HCl removal from **11c** has been shown to be a 16-electron amido-complex. The reductive elimination from the amido complex to an aryl amine complex via a transition state has been investigated. The transition state has been verified by frequency and IRC calculations and the energy barrier of this step has been calculated to be 64 kJ mol^{-1}. This is a lower barrier than the oxidative addition of the aryl halide confirming the latter as the rate determining step in the cycle.

The oxidative addition of chloromethane to the mono-carbene palladium complex was also investigated. A transition state for this process was found to be higher in energy than that for oxidative addition of the aryl chloride and therefore significantly less favoured.

Acknowledgements

We thank Professors Cloke and Caddick for drawing our attention to this problem and for stimulating discussions. We thank the Oxford Supercomputing Centre for computational resources and software support.

References

[1] J.F. Hartwig, Angew. Chem. Int. Ed. 37 (1998) 2046.
[2] R.M. Kissling, M.S. Viciu, G.A. Grasa, R.F. Germaneau, T. Gueveli, M.-C. Pasareanu, O. Navarro-Fernandez, S.P. Nolan, ACS Symp. Ser. 856 (2003) 323.
[3] N. Miyaura, A. Suzuki, Chem. Rev. 95 (1995) 2457.
[4] I.P. Beletskaya, A.V. Cheprakov, Chem. Rev. 100 (2000) 3009.
[5] J.K. Stille, Angew. Chem. Int. Ed. 25 (1986) 508.
[6] C. Amatore, A. Jutand, Acc. Chem. Res. 33 (2000) 314.
[7] S.P. Stambuli, M. Buhl, J.F. Hartwig, J. Am. Chem. Soc. 124 (2002) 9346.
[8] M. Portnoy, D. Milstein, Organometallics 12 (1993) 9346.
[9] E. Galardon, S. Ramdeehul, J.M. Brown, A. Cowley, K.K.M. Hii, A. Jutand, Angew. Chem. Int. Ed. 41 (2002) 1760.
[10] G.A. Grasa, S.V. Milhai, J. Huang, S.P. Nolan, J. Org. Chem. 66 (2001) 7729.
[11] S.R. Stauffer, S. Lee, J.P. Stambuli, S.I. Hauck, J.F. Hartwig, Org. Lett. 2 (2000) 1423.
[12] J. Louie, F. Paul, J.F. Hartwig, Organometallics 15 (1996) 2794.
[13] S. Caddick, F.G.N. Cloke, G.K.B. Clentsmith, P.B. Hitchcock, D. McKerrecher, L.R. Titcomb, M.R.V. Williams, J. Organomet. Chem. 617 (2001) 635.
[14] L.R. Titcomb, S. Caddick, F.G.N. Cloke, D.J. Wilson, D. McKerrecher, Chem. Commun. (2001) 1388.
[15] S. Caddick, F.G.N. Cloke, P.B. Hitchcock, J. Leonard, A.K.d.K. Lewis, D. McKerrecher, L.R. Titcomb, Organometallics 21 (2002) 4318.
[16] A.K.d.K. Lewis, S. Caddick, F.G.N. Cloke, N.C. Billingham, P.B. Hitchcock, J. Leonard, J. Am. Chem. Soc. 125 (2003) 10066.
[17] P.L. Arnold, F.G.N. Cloke, T. Geldbach, P.B. Hitchcock, Organometallics 18 (1999) 3228.
[18] Q. Liu, H.-B. Song, F.-B. Xu, Q.-S. Li, X.-S. Zeng, X.-B. Leng, Z.-Z. Zhang, Polyhedron 22 (2003) 1515.
[19] V.P.W. Bohm, C.W.K. Gstottmayr, T. Weskamp, W.A. Herrmann, J. Organomet. Chem. 595 (2000) 186.
[20] M.S. Viciu, O. Navarro, R.F. Germaneau, R.A. Kelly III, W. Sommer, N. Marion, E.D. Stevens, L. Cavallo, S.P. Nolan, Organometallics 23 (2004) 1629.
[21] J.C. Green, R.G. Scurr, P.L. Arnold, F.G.N. Cloke, Chem. Commun. 1997 (1997) 1963.
[22] J.C. Green, B.J. Herbert, Dalton Trans. (2005) 1214.
[23] A. Sundermann, O. Uzan, J.M.L. Martin, Chem. Eur. J. 7 (2001) 1703.
[24] M. Jakt, L. Johanissen, H.S. Rzepa, D.A. Widdowson, R. Wilhelm (2002) 576.
[25] H.M. Senn, T. Zeigler, Organometallics 23 (2004) 2980.
[26] L.J. Goosen, D. Koley, H.L. Herman, W. Thiel, Organometallics 24 (2005) 2398.
[27] L.J. Goossen, D. Koley, H. Hermann, W. Thiel, Chem. Commun. (2004) 2141.
[28] T.R. Cundari, J. Deng, J. Phys. Org. Chem. 18 (2004) 417.
[29] B.H. Yang, S.L. Buchwald, J. Organomet. Chem. 576 (1999) 125.
[30] J.P. Wolfe, S. Wagaw, J.F. Marcoux, S.L. Buchwald, Acc. Chem. Res. 31 (1998) 805.
[31] J.P. Wolfe, H. Tomori, J.P. Sadighi, J. Yin, S.L. Buchwald, J. Org. Chem. 65 (2000) 1158.
[32] S.A. Macgregor, G.W. Neave, C. Smith, Faraday Discuss. 124 (2003) 111.
[33] K. Albert, P. Gisdakis, N. Rosch, Organometallics 17 (1998) 1608.
[34] W.A. Herrmann, V.P.W. Bohm, C.-P. Reisinger, J. Organomet. Chem. 576 (1999) 23.
[35] H.C. Brown, P. Heim, J. Org. Chem. 38 (1973) 912.
[36] H.C. Brown, Y.O.N.G.M. Choi, Synthesis 8 (1981) 605.
[37] F. Rolla, J. Org. Chem. 47 (1982) 4327.
[38] A.W. Hofmann, Ber. 14 (1881) 2725.
[39] T. Curtius, Ber. 23 (1880) 275.

[40] G.W.T.M.J. Frisch, H.B. Schlegel, G.E. Scuseria, J.R.C.M.A. Robb, V.G. Zakrzewski, J.A. Montgomery Jr., J.C.B.R.E. Stratmann, Dapprich, J.M. Millam, K.N.K.A.D. Daniels, M.C. Strain, O. Farkas, J. Tomasi, M.C.V. Barone, R. Cammi, B. Mennucci, C. Pomelli, C. Adamo, J.O.S. Clifford, G.A. Petersson, P.Y. Ayala, Q. Cui, P.S.K. Morokuma, J.J. Dannenberg, D.K. Malick, K.R.A.D. Rabuck, J.B. Foresman, J. Cioslowski, A.G.B.J.V. Ortiz, B.B. Stefanov, G. Liu, A. Liashenko, I.K.P. Piskorz, R. Gomperts, R.L. Martin, D.J. Fox, M.A.A.-L.T. Keith, C.Y. Peng, A. Nanayakkara, M. Challacombe, B.J.P.M.W. Gill, W. Chen, M.W. Wong, J.L. Andres, M.H.-G.C. Gonzalez, E.S. Replogle, J.A. Pople, Revision A.2.1 ed., Gaussian Inc., Pittsburgh, PA, 2003.
[41] S.H. Vosko, L. Wilk, M. Nusair, Can. J. Phys. 58 (1980) 1200.
[42] A.D. Becke, Phys. Rev. A 38 (1988) 3098.
[43] J.P. Perdew, Phys. Rev. B 33 (1986) 8800.
[44] D. Andrae, U. Haeussermann, M. Dolg, H. Stoll, H. Preuss, Theor. Chim. Acta 78 (1991) 247.
[45] D. Andrae, U. Haeussermann, M. Dolg, H. Stoll, H. Preuss, Theor. Chim. Acta 77 (1990) 123.
[46] R. Ditchfield, W.J. Hehre, J.A. Pople, J. Chem. Phys. 54 (1971) 724.
[47] W.J. Hehre, R. Ditchfield, J.A. Pople, J. Chem.Phys. 56 (1972) 2257.
[48] P.C. Hariharan, J.A. Pople, Theor. Chim. Acta 28 (1973) 213.
[49] M.M. Francl, W.J. Pietro, W.J. Hehre, J.S. Binkley, M.S. Gordon, D.J. DeFrees, J.A. Pople, J. Chem. Phys. 77 (1982) 3654.
[50] V.A. Rassolov, J.A. Pople, M.A. Ratner, T.L. Windus, J. Chem. Phys. 109 (1998) 1223.
[51] V.A. Rassolov, M.A. Ratner, J.A. Pople, P.C. Redfern, L.A. Curtiss, J. Comput. Chem. 22 (2001) 976.
[52] T.H. Dunning Jr., J. Chem. Phys. 90 (1989) 1007.
[53] R.A. Kendall, T.H. Dunning Jr., R.J. Harrison, J. Chem. Phys. 96 (1992) 6796.
[54] D.E. Woon, T.H. Dunning Jr., J. Chem. Phys. 98 (1993) 1358.
[55] S. Miertus, E. Scrocco, J. Tomasi, Chem. Phys. 55 (1981) 117.
[56] S. Miertus, J. Tomasi, Chem. Phys. 65 (1982) 239.
[57] B. Mennucci, J. Tomasi, J. Chem. Phys. 106 (1997) 5151.
[58] M. Cossi, V. Barone, R. Cammi, J. Tomasi, Chem. Phys. Lett. 255 (1996) 327.